

# Tribological Properties of Oleylamine-Modified Ultrathin WS<sub>2</sub> Nanosheets as the Additive in Polyalpha Olefin Over a Wide Temperature Range

Zhengquan Jiang<sup>1</sup> · Yujuan Zhang<sup>1</sup> · Guangbin Yang<sup>1</sup> · Kunpeng Yang<sup>1</sup> · Shengmao Zhang<sup>1</sup> · Laigui Yu<sup>1</sup> · Pingyu Zhang<sup>1</sup>

Received: 19 August 2015 / Accepted: 13 January 2016  
© Springer Science+Business Media New York 2016

**Abstract** Ultrathin WS<sub>2</sub> nanosheets modified by oleylamine (OM) were prepared via a solution-phase method at a relatively high temperature of 300 °C. The thermal stability of the as-prepared WS<sub>2</sub> nanosheets was evaluated by thermogravimetric analysis. The tribological properties of as-synthesized WS<sub>2</sub> nanosheets as the additive in polyalpha olefin (PAO6) were evaluated with a four-ball machine and a reciprocating tribometer over a wide temperature range from room temperature to 200 °C. The morphology and elemental composition of worn steel surfaces were analyzed with a scanning electron microscope, a three-dimensional optical profiler, an energy dispersive spectrometer and an X-ray photoelectron spectroscopy. Results show that OM as the modifier is able to improve the dispersibility of WS<sub>2</sub> nanosheets in PAO6 base oil. At a mass fraction of 2.0 % in PAO6 base oil, as-synthesized WS<sub>2</sub> nanosheets exhibit excellent antiwear and friction-reducing performance over the selected temperature range. This is because as-synthesized WS<sub>2</sub> nanosheets as the additive in PAO6 are able to form adsorbed film with a low shear force and tribochemical reaction film composed of W, Fe and O elements on the worn steel surface.

**Keywords** WS<sub>2</sub> nanosheet · Polyalpha olefin · Lubricant additive · Tribological properties

## 1 Introduction

About one third to one half of the world's primary energy is dissipated in mechanical friction, and 80 % of machinery component failure is caused by wear [1–3]. To deal with these issues, researchers have made great efforts to develop various lubricant additives thereby saving energy and increase the reliability of machinery components via effectively reducing friction and wear. Among various lubricant additives, nano-materials are of particular significance, since they exhibit advantages including low dosage, better anti-friction resistance and wear resistance performance [3–10].

Layer-lattice solids such as graphite, molybdenum disulfide and tungsten disulfide are traditional solid lubricants, since they shear easily [11]. For example, conventional tungsten disulfide has a characteristic anisotropic layered structure consisting of W–S atoms covalently bonded in planar hexagonal arrays; each of its W atom is surrounded by a trigonal prism of S atoms within a lamella while adjacent lamellae interact through relatively weak van der Waals forces to allow the layers to slip under a small shear force [12].

Similar to conventional tungsten disulfide, nanometer WS<sub>2</sub> has a multi-layered structure and exists in plate-like (2H) and inorganic fullerene-like (IF) forms [13]. This is why nanometer WS<sub>2</sub> as a lubricant additive suitable to harsh conditions is of particular significance [12–20]. Aldana et al. [14] studied the tribological properties of nanometer 2H-WS<sub>2</sub> as an additive in polyalpha olefin (PAO) base oil and found that nano-WS<sub>2</sub> can react with metal substrate to generate tribofilms with a layered structure and excellent tribological properties. Joly-Pottuz et al. [16] reported that nanoscale IF-WS<sub>2</sub> as a lubricating oil additive can effectively reduce friction and wear under

✉ Shengmao Zhang  
zsm@henu.edu.cn

<sup>1</sup> Engineering Research Center for Nanomaterials, Henan University, Kaifeng 475004, People's Republic of China

boundary lubrication condition. An et al. [20] found that nanolamellar tungsten and molybdenum disulfides display better friction-reducing and antiwear properties than micro-sized counterparts.

It is widely accepted that the lubrication properties of nanoparticles as lubricant additives are attributed to a gradual exfoliation of the external sheets of the particles during friction process leading to their transfer onto the asperities of the reciprocating surfaces [3, 14]. It is usually required that lubricant additives work well over a wide range of temperature [21], and 150 °C is specified as the moderately high temperature for automotive engine oil [22]. Unfortunately, extreme lubricating temperatures can often exceed the thermal degradation limits of many lubricating oils and lubricant additives. Therefore, it is imperative to develop low-cost lubricating oil additives that can provide excellent friction-reducing and antiwear properties over a wide temperature range, especially at elevated temperature.

The present research aims to elucidate the lubrication properties of WS<sub>2</sub> nanosheets over a wide temperature (from room temperature to 200 °C) and reveal their action mechanisms in relation to analysis of the tribofilm generated on worn steel surfaces. This article reports the preparation of ultrathin WS<sub>2</sub> nanosheets modified by oleylamine [23] and the valuation of the tribological properties of the as-prepared WS<sub>2</sub> nanosheets as lubricant additive in PAO.

## 2 Experiment

### 2.1 Preparation of Ultrathin WS<sub>2</sub> Nanosheets Modified by Oleylamine

Ultrathin WS<sub>2</sub> nanosheets modified by oleylamine (OM) were synthesized by high-temperature solution-phase method reported elsewhere [23]. Figure 1 schematically shows the route to synthesizing WS<sub>2</sub> nanosheets. Briefly, WCl<sub>6</sub> (1 mmol) was added into the mixture of OM (20 mL) and 1-octadecene (ODE 10 mL) in a three-

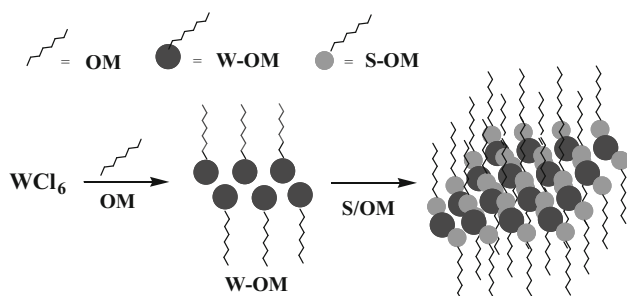


**Fig. 1** Synthesis of ultrathin WS<sub>2</sub> nanosheets modified by OM

necked flask (50 mL). The flask was ultrasonically vibrated for 30 min so that WCl<sub>6</sub> was dissolved completely. Resultant solution was heated to 140 °C and held there for about 30 min to remove water and oxygen under vigorous magnetic stirring in the presence of argon for protection. Then the solution was heated to 300 °C in 15 min and kept there for another 30 min in argon atmosphere, followed by the injection of 5 mL of OM containing 2 mmol of dissolved sulfur powder within 10 min through an injection pump. Upon completion of the injection of the S-dissolved OM, the mixed solution was kept at 300 °C for 60 min to allow the generation of WS<sub>2</sub> nanosheets. At the end of the reaction, the reaction mixture was cooled down to room temperature and ultrasonically cleaned with excess absolute ethanol, followed by centrifugation to remove organic residue and afford WS<sub>2</sub> nanosheets modified by OM.

### 2.2 Characterization of Ultrathin WS<sub>2</sub> Nanosheets Modified by Oleylamine

X-ray powder diffraction (XRD) patterns were collected with an X'Pert Pro diffractometer (Cu K $\alpha$  radiation,  $\lambda = 0.15418$  nm; 40 kV, 40 mA). Transmission electron microscopy (TEM) images were obtained with a JEM-2010 microscope. A drop of the solution of as-prepared ultrathin WS<sub>2</sub> nanosheets in absolute ethanol was placed on a copper grid covered by carbon film and dried completely at ambient temperature to obtain the sample for TEM analysis.

### 2.3 Evaluation of Thermal Stability and Tribological Properties of Ultrathin WS<sub>2</sub> Nanosheets Modified by Oleylamine

Camera pictures of the dispersions of the OM-modified WS<sub>2</sub> nanosheets in PAO6 base oil under different storage conditions were taken to estimate their dispersion stability, where the dispersion of the as-prepared OM-modified WS<sub>2</sub> nanosheets, the same dispersion after 6 months of storage at ambient condition and the dispersion of the as-prepared OM-modified WS<sub>2</sub> nanosheets after being stored in an electric drying oven (Tianjin Taisite Machine Factory, Tianjin, China) at 160 °C for 7 days were separately tested. Thermogravimetric analysis (TGA) was conducted with a DSC6200 thermal analyzer at a scanning rate of 10 °C/min in an air flow.

The antioxidation behavior of WS<sub>2</sub> nanosheets modified by oleylamine was evaluated by rotary oxygen bomb test (denoted as ROBT). A proper amount of as-synthesized target product, together with a proper amount of water and a copper catalyst coil, was sealed in the rotary bomb and then charged with oxygen at a pressure of 620 kPa under

room temperature. The rotary bomb was then placed in a dimethyl silane heating bath at a constant temperature of 150 °C. Oxidation stability is expressed as the time required for achieving a specified pressure drop of 175 kPa.

The tribological properties of OM-modified WS<sub>2</sub> nanosheets as additive in PAO6 base oil were evaluated with a four-ball machine. GCr15 bearing steel (SAE-52100) balls with a diameter of 12.7 mm and a hardness of HRC 61–64, purchased from Shanghai Bearing Factory (Shanghai, China), were used to assemble the sliding pair. The friction and wear tests were conducted at a rotary speed of 1200 rev/min and a load of 92, 192, 292, 392 and 492 N from ambient temperature to 200 °C for a duration of 60 min. At the end of each test, the wear scar diameter (WSD) on the three lower balls was measured with an optical microscope at an accuracy of 0.01 mm. The friction coefficient was recorded by a computer attached to the friction and wear tester. The friction and wear tests under each pre-set condition were repeated three times (relative deviation for WSD is ±5.0 % and the deviation of the friction coefficient is ±0.004). The average wear scar diameter of the three lower balls is calculated and reported in this paper. The  $P_B$  (maximum non-seizure load, the last load at which the measured wear scar diameter is not more than 5 % greater than the compensation value at that load) values of PAO6 and PAO6 containing as-prepared additive were evaluated according to Chinese national standard method GB/T 3142-82 (similar to ASTM D 2783-1998). The physicochemical properties of base oil PAO6 are given in Table 1.

The morphology of worn steel surfaces was observed with a JSM-5600 scanning electron microscope (SEM), and the wear volume was measured with a three-dimensional (3D) optical profiler (Bruker, Contour GT-I 3D). Energy dispersive spectrometry (EDS) and X-ray photoelectron spectroscopy (XPS) were performed to determine the elemental composition and chemical states of some typical elements in the worn surfaces of the steel balls. Prior to EDS and XPS analyses, the steel balls were

cleaned with acetone in an ultrasonic bath and fully dried in atmosphere to remove any contaminants.

The Stribeck curves of base oil PAO6 and the base oil containing 2.0 % (mass fraction) OM-modified WS<sub>2</sub> additive were recorded with a high-frequency reciprocating friction and wear tester. Four major lubrication states, including boundary lubrication, mixed lubrication, elasto-hydrodynamic lubrication and hydrodynamic lubrication, can be identified according to the Stribeck curve [24], and the Stribeck curve can be adopted to effectively evaluate the lubricating performance of various lubricants and simulate the actual working condition. The friction and wear tests were performed in a ball-on-disk contact geometry to measure the Stribeck curves. The GCr15 bearing steel ball (Poisson ratio: 0.3, elastic modulus: 208 GPa, diameter: 4 mm) and AISI A390 aluminum alloy [20 mm × 20 mm; Poisson ratio: 0.300, elastic modulus: 77 GPa, composition: 76.2 % Al (deviation ±0.33, atomic fraction; the same hereafter), 16.16 % Si (±0.12), 0.36 % Fe (±0.02), 0.11 % Ti (±0.03), 4.39 % Cu (±0.04), 0.11 % Zr (±0.03), 2.25 % Ni (±0.03)] were adopted to assemble the ball-on-disk sliding pair. The ball-on-disk sliding tests were conducted at a stroke of 10 mm, a series of normal load ( $F_N$ ) and frequency, a temperature of about 20, 75, 150, and 200 °C, and a duration of 220 min while the lubricating oil was added to the oil box to fully immerse the lower steel ball as the disk reciprocally slid. The friction coefficient was recorded by a computer attached to the high-frequency reciprocating test rig. The sliding tests under each pre-set condition were repeated three times, and the deviation of the friction coefficient is ±0.004. The averages of the repeat tests were calculated and reported in the Stribeck curves.

### 3 Result and Discussion

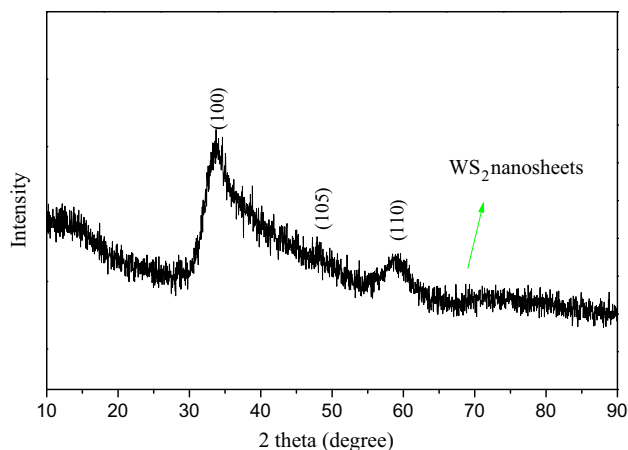
#### 3.1 TEM and XRD Analyses of WS<sub>2</sub> Nanosheets Modified by Oleylamine

Figure 2 shows the XRD pattern of as-prepared WS<sub>2</sub> nanosheets modified by OM. The XRD pattern of the annealed OM-modified WS<sub>2</sub> nanosheets is similar to that reported elsewhere [23]; and both the (100) and (110) peaks exhibit an apparent asymmetry, which is attributed to the turbostratic stacking of layered compounds. Besides, OM-modified WS<sub>2</sub> nanosheets belong to 2H polytype of platelets and exhibit poor crystallinity.

Figure 3 shows the TEM images of OM-modified WS<sub>2</sub> nanosheets. It can be seen that the as-prepared OM-modified WS<sub>2</sub> nanosheets exhibit an average particle size of 6–8 nm and belong to 2H polytype of platelets, which is in accordance with the above-mentioned XRD analysis.

**Table 1** Physicochemical properties of PAO6 oil

Item	Value
Density at 15.6 °C	0.826 g/cm
Kinematic viscosity at 40 °C	30.60 ± 0.01 mm <sup>2</sup> /s
Kinematic viscosity at 100 °C	5.90 ± 0.002 mm <sup>2</sup> /s
Viscosity index	135
Average molecular weight	513 ± 10
Pour point	−68 °C
Degradation temperatures (50 % mass loss)	295.2 °C



**Fig. 2** XRD pattern of OM-modified WS<sub>2</sub> nanosheets

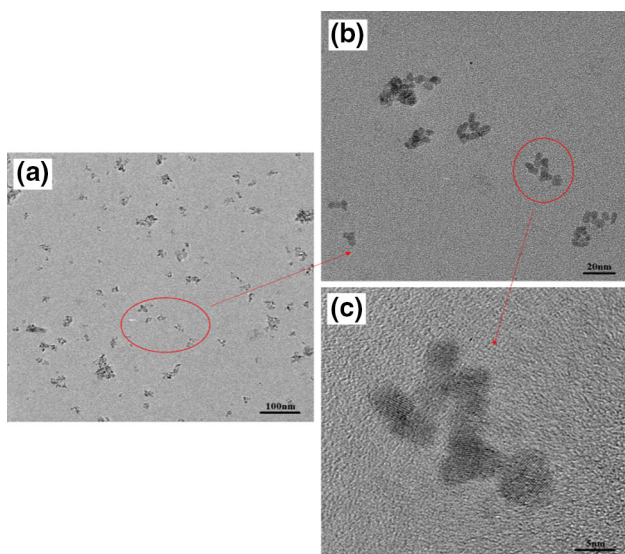


**Fig. 3** TEM images of OM-modified WS<sub>2</sub> nanosheets under different magnifications (**a** 25,000 $\times$ , **b** 10,000 $\times$ , **c** 500,000 $\times$ )

### 3.2 Dispersivity as Well as Thermal Stability and Antioxidation Behavior of OM-Modified WS<sub>2</sub> Nanosheets

Figure 4 shows the camera pictures of the dispersions of as-synthesized WS<sub>2</sub> nanosheets modified by OM in PAO6 base oil after storage under different conditions. Both the dispersion of the as-prepared OM-modified WS<sub>2</sub> nanosheets and the one after 6 months of storage at ambient condition appear to be black and exhibit good dispersion stability (see Fig. 4a, b). After being stored in the oven at 160 °C for 7 days, the dispersion turns red but still retains good stability. This indicates that the OM-modified WS<sub>2</sub> nanosheets exhibit good dispersion stability in PAO6 base

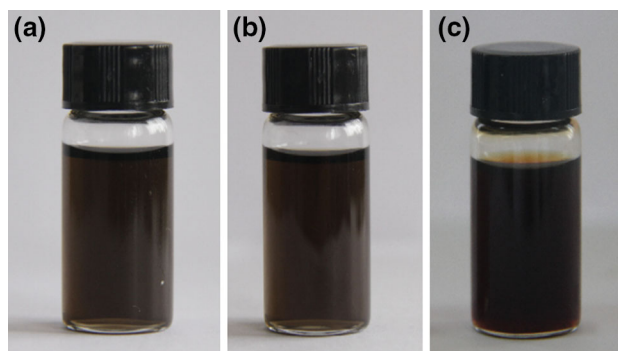


**Fig. 4** Camera pictures of WS<sub>2</sub> nanosheets dispersed in PAO6 oil: **a** dispersion of as-synthesized product, **b** dispersion of the as-synthesized product after a storage of 6 months and **c** dispersion of the as-synthesized product after storage in an electric drying oven at 160 °C for 7 days

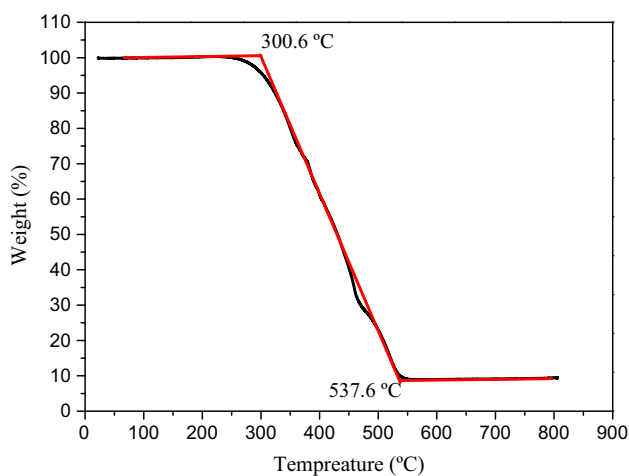


**Fig. 5** TGA curve of OM-modified WS<sub>2</sub> nanosheets

oil at room temperature and moderately elevated temperature as well.

Figure 5 shows the TGA curve of the OM-modified WS<sub>2</sub> nanosheets. It can be seen that the OM-modified WS<sub>2</sub> nanosheets remain almost unchanged from room temperature to 300.6 °C. The OM-modified WS<sub>2</sub> nanosheets undergo the initial stage of weight loss at 300.6 °C and turn dark in color. Besides, the complete thermal decomposition of the OM-modified WS<sub>2</sub> nanosheets occurs around 537.6 °C, and at this temperature a residue of about 9.47 % (mass fraction) remains, possibly corresponding to WO<sub>3</sub> and a small amount of amorphous carbon that are favorable for reducing friction and wear [25–27].

Figure 6 shows the oxidation induction time of PAO6 base oil and the base oil containing 2 % (mass fraction) WS<sub>2</sub> nanosheets determined by ROBT. The oxidation induction time of PAO6 base oil is 45 min, and the

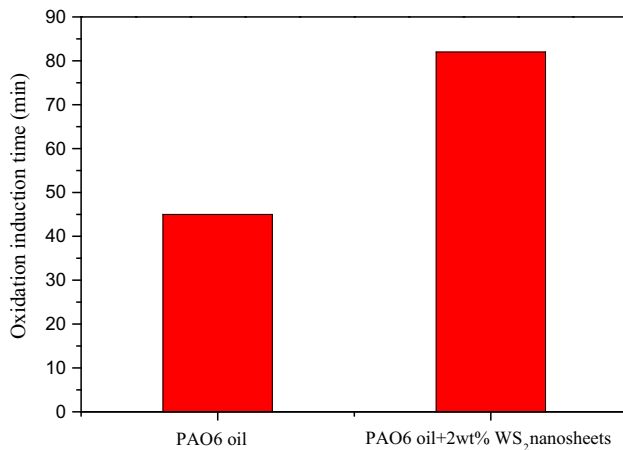


**Fig. 6** Oxidation induction time of PAO6 oil and PAO6 with 2.0 % (mass fraction) WS<sub>2</sub> nanosheets

introduction of the OM-modified WS<sub>2</sub> nanosheets significantly increases the oxidation induction time to 82 min. This indicates that the OM-modified WS<sub>2</sub> nanosheets are able to effectively slow down the oxidation process of PAO6.

### 3.3 Tribological Properties of As-prepared WS<sub>2</sub> Nanosheets as Additive in PAO6 Oil Over a Wide Temperature Range

Figures 7 and 8 show the variations in the friction coefficients and wear scar diameters with the concentration of OM-modified WS<sub>2</sub> nanosheets in PAO6 base oil (load: 392 N; speed: 1200 rev/min; time: 60 min; temperature: 75 °C). It can be seen that the OM-modified WS<sub>2</sub>

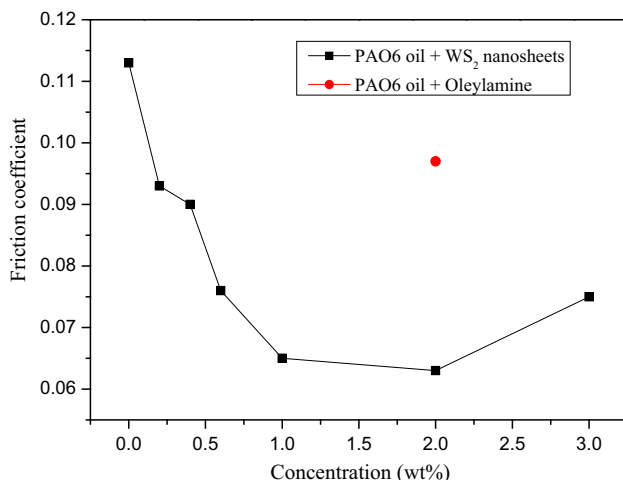


**Fig. 7** Variation in friction coefficient with concentration of OM-modified WS<sub>2</sub> nanosheets in PAO6

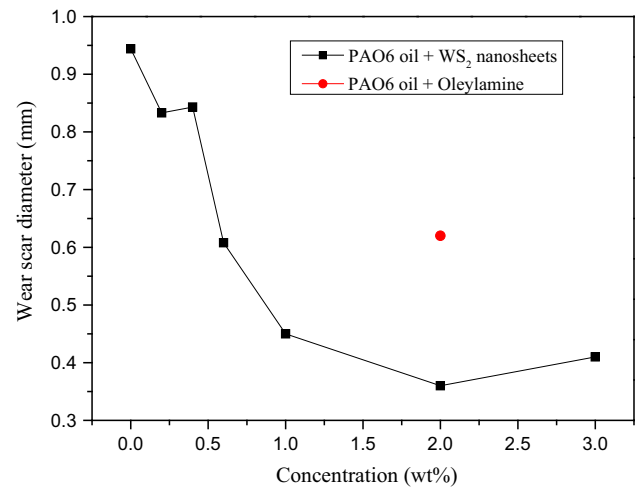


**Fig. 8** Variation in WSD with concentration of WS<sub>2</sub> nanosheets in PAO6

nanosheets as an additive in PAO6 base oil are effective in reducing the friction coefficient and wear scar diameter of the steel–steel pair. Namely, when 2.0 % (mass fraction; the same hereafter) of WS<sub>2</sub> nanosheets is added into PAO6, the best antiwear performance and friction-reducing ability are obtained: The wear scar diameter is decreased from 0.944 to 0.360 mm, and the friction coefficient is decreased from 0.113 to 0.063 (corresponding to a reduction by 61.9 and 44.2 %). However, higher concentrations of WS<sub>2</sub> nanosheets in PAO6 oil lead to increase in the friction coefficient and wear scar diameter: As the additive concentration is above 2.0 %, both the friction coefficient and wear scar diameter tend to slightly rise with increasing additive concentration. Moreover, OM-modified WS<sub>2</sub> nanosheets as the additive are advantageous over oleylamine (PAO6 oil containing 2 % OM provides a friction coefficient of 0.098 and a wear scar diameter of 0.620 mm). It can be inferred that, at a too low additive concentration, the lubricant can hardly form a tribofilm with good coverage to prevent the direct contact of the sliding steel pairs, thereby leading to relatively high friction coefficient. When the additive concentration is too high, the OM-modified WS<sub>2</sub> nanosheets would tend to form large aggregates and cannot properly fill the valleys between the asperities of the sliding steel pair, thereby also yielding a relatively high friction coefficient in association with enhanced scratching and shearing [28, 29]. Therefore, it is suggested to keep the concentration of the OM-modified WS<sub>2</sub> in PAO6 as 2.0 % in order to effectively reduce the friction and wear of the steel–steel sliding pair.

Figure 9 shows the friction coefficient–time curves of PAO6 oil and PAO6 oil containing 2.0 % of OM-modified WS<sub>2</sub> nanosheets under 75 °C (load: 392 N; speed: 1200 rev/min; time: 60 min). The friction curve of the

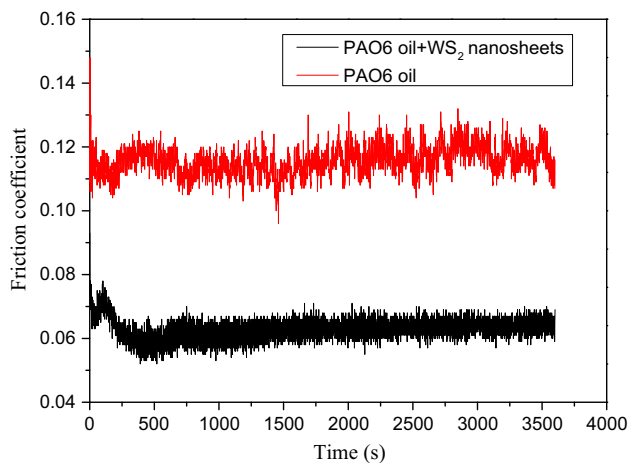


**Fig. 9** Friction curves of PAO6 oil and PAO6 oil containing 2.0 % of OM-modified WS<sub>2</sub> nanosheets under 75 °C

PAO6 base oil containing 2.0 % WS<sub>2</sub> nanosheets additive stays always below that of the PAO6 base oil, which demonstrates that the additive can effectively improve the friction-reducing ability of the base oil. Besides, the friction coefficient under the lubrication of PAO6 base oil containing 2.0 % WS<sub>2</sub> nanosheets tends to slightly increase with extending sliding time, which is possibly because a part of the tungsten disulfide additives is gradually oxidized during the sliding process.

Figures 10 and 11 show the variation of wear scar diameter and friction coefficient with temperature under the lubrication of PAO6 oil containing 2.0 % of WS<sub>2</sub> nanosheets (load: 392 N; speed: 1200 rev/min; time: 60 min; temperature: from ambient temperature to 200 °C). It is seen that WS<sub>2</sub> nanosheets as the additive can effectively improve the friction-reducing and antiwear

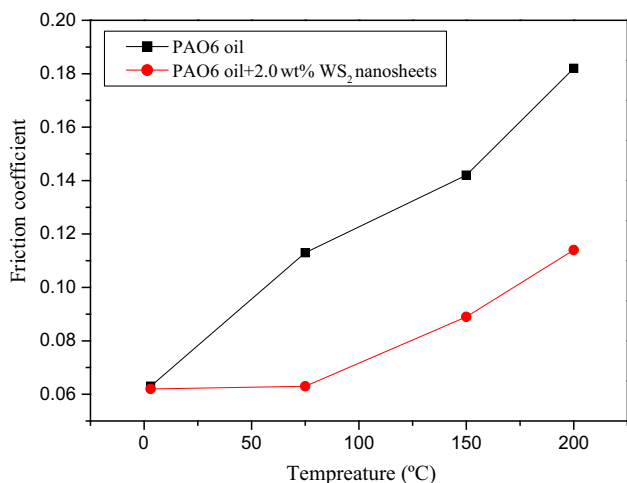


**Fig. 10** Variation of friction coefficient with temperature

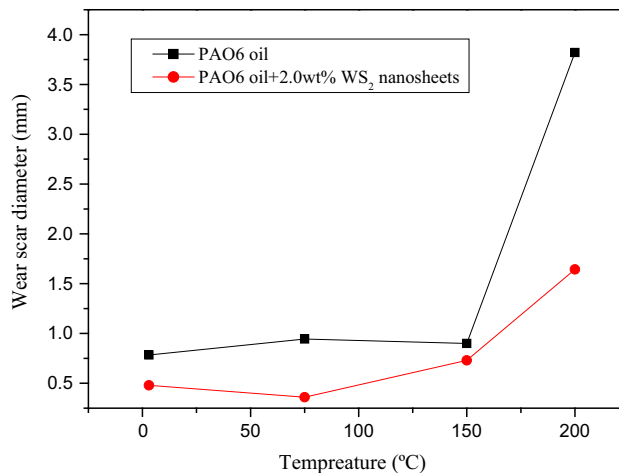


**Fig. 11** Variation of wear scar diameter with temperature

**Table 2** Variation of wear volume with temperature

Temperature (°C)	Wear volume under the lubrication of PAO6 oil (μm <sup>3</sup> )	Wear volume under the lubrication of PAO6 with WS <sub>2</sub> nanosheets (μm <sup>3</sup> )
Room	4.10 × 10 <sup>6</sup>	9.57 × 10 <sup>5</sup>
75	1.60 × 10 <sup>7</sup>	6.92 × 10 <sup>5</sup>
150	1.27 × 10 <sup>8</sup>	3.54 × 10 <sup>6</sup>
200	3.32 × 10 <sup>9</sup>	1.25 × 10 <sup>8</sup>

abilities as well as load-carrying capacity of PAO6 base oil. In the meantime, the wear scar diameter and friction coefficient of the steel–steel pair considerably increase with increasing temperature. For example, the friction coefficient under the lubrication of PAO6 oil containing 2.0 % of WS<sub>2</sub> nanosheets is 0.089 and 0.114 when the temperature reaches 150 and 200 °C, lower than that under the lubrication of PAO6 alone. Similarly, the wear scar diameter of the steel–steel contact lubricated by PAO6 oil containing 2.0 % of WS<sub>2</sub> nanosheets at 150 and 200 °C is 0.731 and 1.643 mm, also smaller than that of the steel sliding pair lubricated by PAO6 alone.

The variation in the wear volume with temperature under the lubrication of PAO6 oil containing 2.0 % of WS<sub>2</sub> nanosheets (speed: 1200 rev/min; time: 60 min; temperature: from ambient temperature to 200 °C) is listed in Table 2. Similar to what is observed for wear scar diameter, WS<sub>2</sub> nanosheets as the additive can effectively improve the antiwear ability of PAO6 base oil from room temperature to 200 °C.

Figures 12 and 13 show the variations of wear scar diameter and friction coefficient with load under the lubrication of PAO6 oil and PAO6 oil containing 2.0 wt%

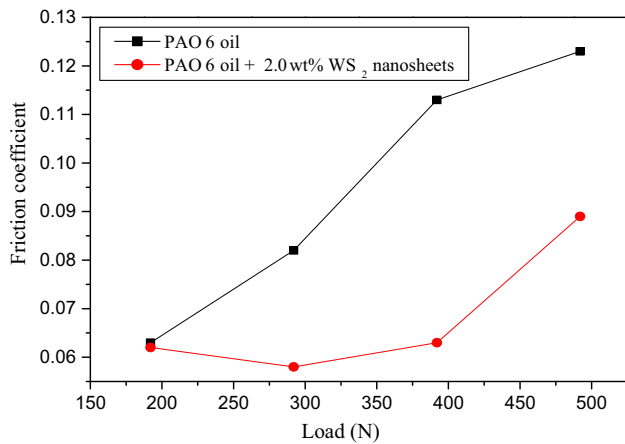


Fig. 12 Variation of friction coefficient with load

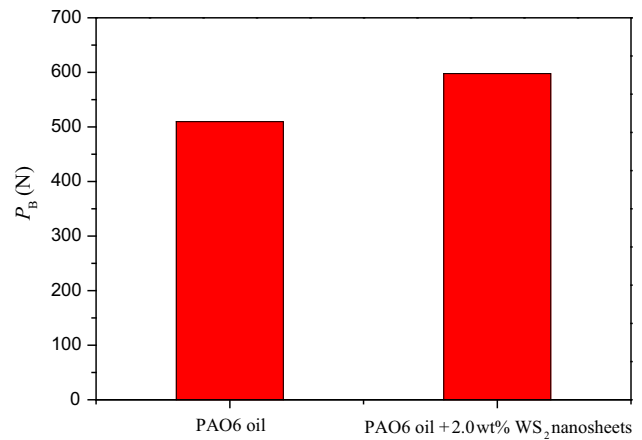


Fig. 14 P<sub>B</sub> value of PAO6 oil and PAO6 oil containing 2.0 % WS<sub>2</sub> nanosheets

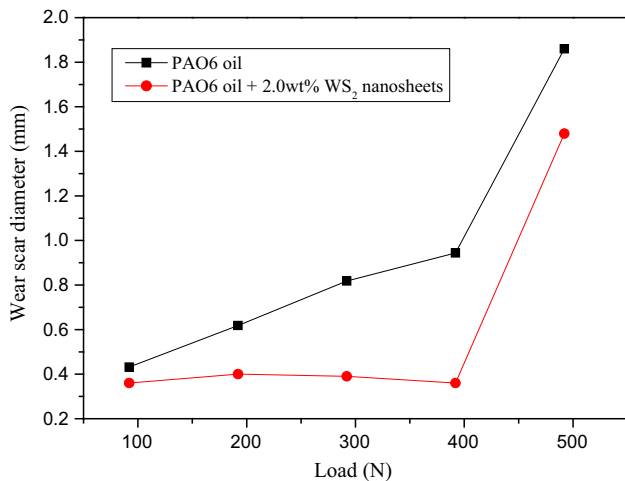


Fig. 13 Variation of wear scar diameter with load

of WS<sub>2</sub> nanosheets (speed: 1200 rev/min; time: 60 min; temperature: 75 °C). It is seen that WS<sub>2</sub> nanosheets can effectively improve the friction-reducing and antiwear abilities of PAO6 oil when the load is below 392 N. The reason may lie in that the stable suspension of WS<sub>2</sub> nanosheets in PAO6 oil can be readily transferred onto the contact zone of rubbing steel surfaces and deposited thereon to form a surface protective and lubricious layer, resulting in reduced friction coefficient and wear scar diameter. As the load increases to 492 N, however, the wear scar diameter rises significantly, which is attributed to the worsening in the tribological behavior of the OM-modified WS<sub>2</sub> additive at a too high load.

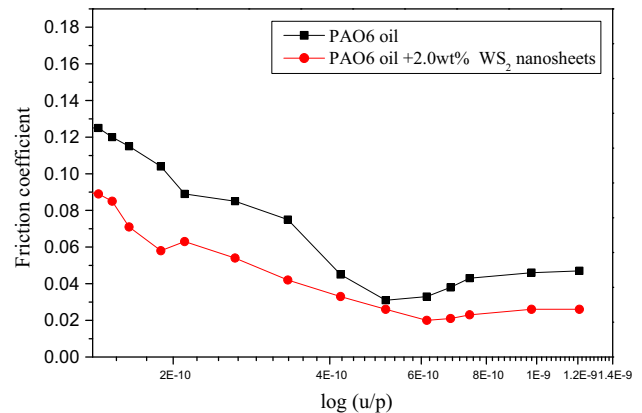


Fig. 15 Stribeck curves of PAO6 oil and PAO6 oil containing 2.0 % of OM-modified WS<sub>2</sub> nanosheets under room temperature

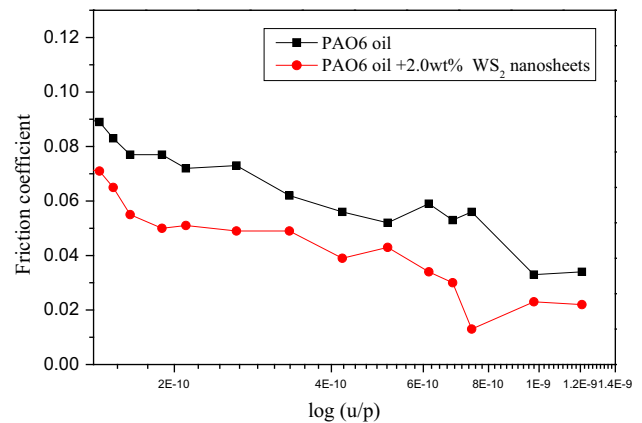
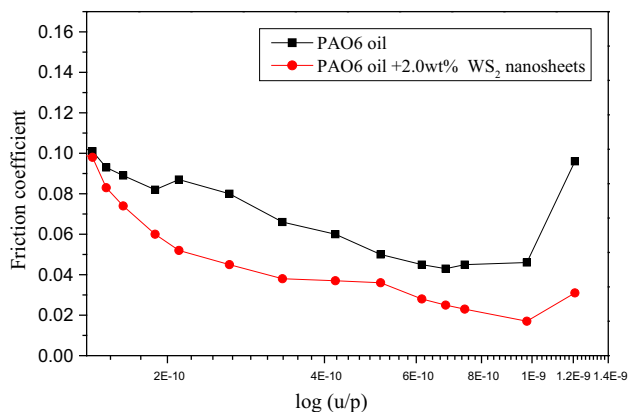
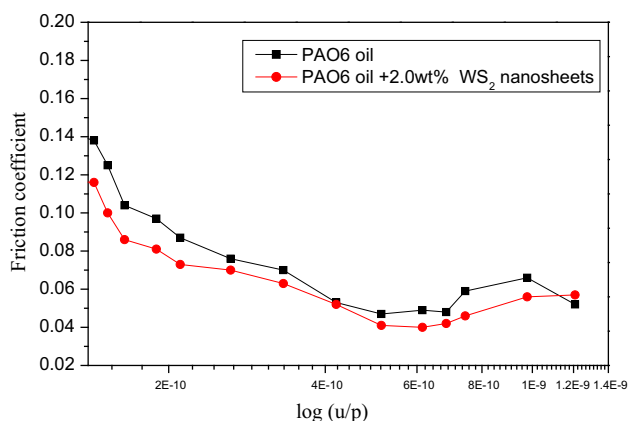


Fig. 16 Stribeck curves of PAO6 oil and PAO6 oil containing 2.0 % of OM-modified WS<sub>2</sub> nanosheets under 75 °C



**Fig. 17** Stribeck curves of PAO6 oil and PAO6 oil containing 2.0 % of OM-modified WS<sub>2</sub> nanosheets under 150 °C



**Fig. 18** Stribeck curves of PAO6 oil and PAO6 oil containing 2.0 % of OM-modified WS<sub>2</sub> nanosheets under 200 °C

The  $P_B$  values of PAO6 oil and PAO6 oil containing 2.0 % WS<sub>2</sub> nanosheets are shown in Fig. 14. It can be seen that the  $P_B$  values of PAO6 oil and PAO6 oil containing 2.0 % WS<sub>2</sub> nanosheets are 509.6 and 597.8 N, which indicates that the OM-modified WS<sub>2</sub> nanosheets as the additive can effectively improve the load-carrying capacity of PAO6.

The Stribeck curves measured with the HFRR test rig under room temperature and various elevated temperatures are shown in Figs. 15, 16, 17, 18. It can be seen that PAO6-2.0 % WS<sub>2</sub> allows the steel–steel sliding pair to enter the

elastohydrodynamic lubrication region earlier than the PAO6 base oil under each of elevated temperatures, but the elastohydrodynamic lubrication behavior of the two kinds of lubricants under ambient temperature seems to be virtually the same. Besides, the Stribeck curves of the PAO6 base oil containing 2.0 % WS<sub>2</sub> nanosheets additive stay always below those of the PAO6 base oil alone, which demonstrates that the former exhibits better friction-reducing ability than the latter in boundary, mixed and elastohydrodynamic lubrication regions, as evidenced by four-ball friction and wear tests.

### 3.4 SEM–EDS and XPS Analyses of Worn Surfaces

Figures 19 and 20 present the SEM images of the wear scar of steel balls lubricated by PAO6 oil and PAO6 oil containing 2.0 % WS<sub>2</sub> nanosheets at temperatures 75 and 150 °C (load: 392 N; speed: 1200 rev/min; time: 60 min). It can be seen that the worn steel surface lubricated by PAO6 alone is quite rough and shows obvious signs of deep furrows and grooves in the sliding direction (Figs. 18a, c, 19a, c). Contrary to the above, the worn steel surfaces lubricated by PAO6 containing 2 % WS<sub>2</sub> nanosheets are smoother and show fewer signs of scratching (Figs. 18b, d, 19b, d), which is indicative of the good antiwear ability of OM-modified WS<sub>2</sub> nanosheets over a wide range of temperature [12–20].

The planar and 3D morphologies of the worn steel surfaces observed with the 3D profiler are shown in Fig. 21. It can be seen that, whether at room temperature or elevated temperature, PAO6 containing 2.0 % OM-modified WS<sub>2</sub> nanosheets additive always provides a smaller wear scar (referring to smaller wear depth and wear volume) of the steel–steel sliding pair than the PAO6 base oil alone. This well corresponds to the observation that the OM-modified WS<sub>2</sub> nanosheets additive can effectively improve the tribological properties of PAO6 base oil in the temperature range of room temperature ~200 °C.

The worn surfaces of the lower steel balls lubricated by PAO6 oil containing 2.0 % WS<sub>2</sub> nanosheets were analyzed by SEM–EDS so as to acquire more information about the deposition of the nanoscale additive on the sliding steel surfaces. As shown in Figs. 22 and 23, the content of S of the contact region is relatively lower than that of the non-

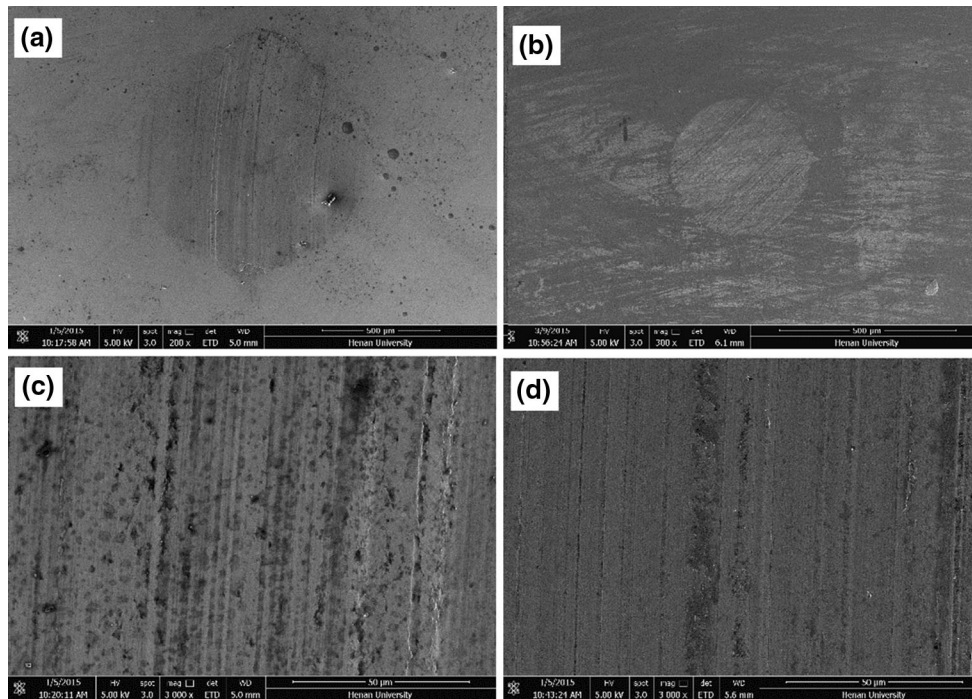


**Fig. 19** SEM micrographs of worn steel ball surfaces lubricated by PAO6 oil **a, c** and PAO6 oil containing 2.0 % of WS<sub>2</sub> nanosheets, **b, d** (load: 392 N; speed: 1200 rev/min; time: 60 min; 75 °C)

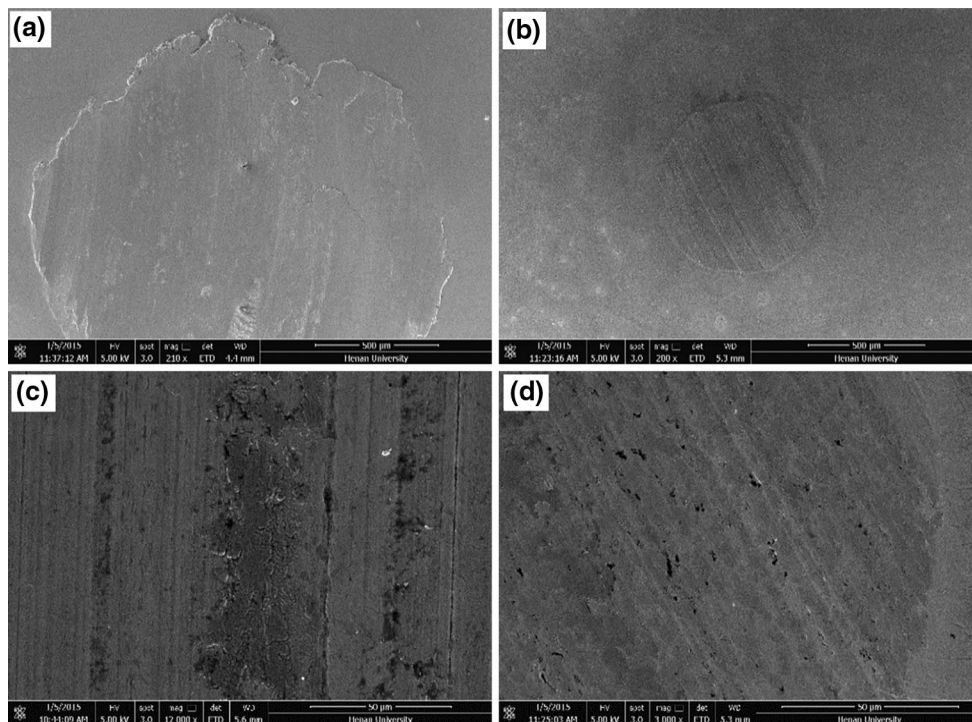
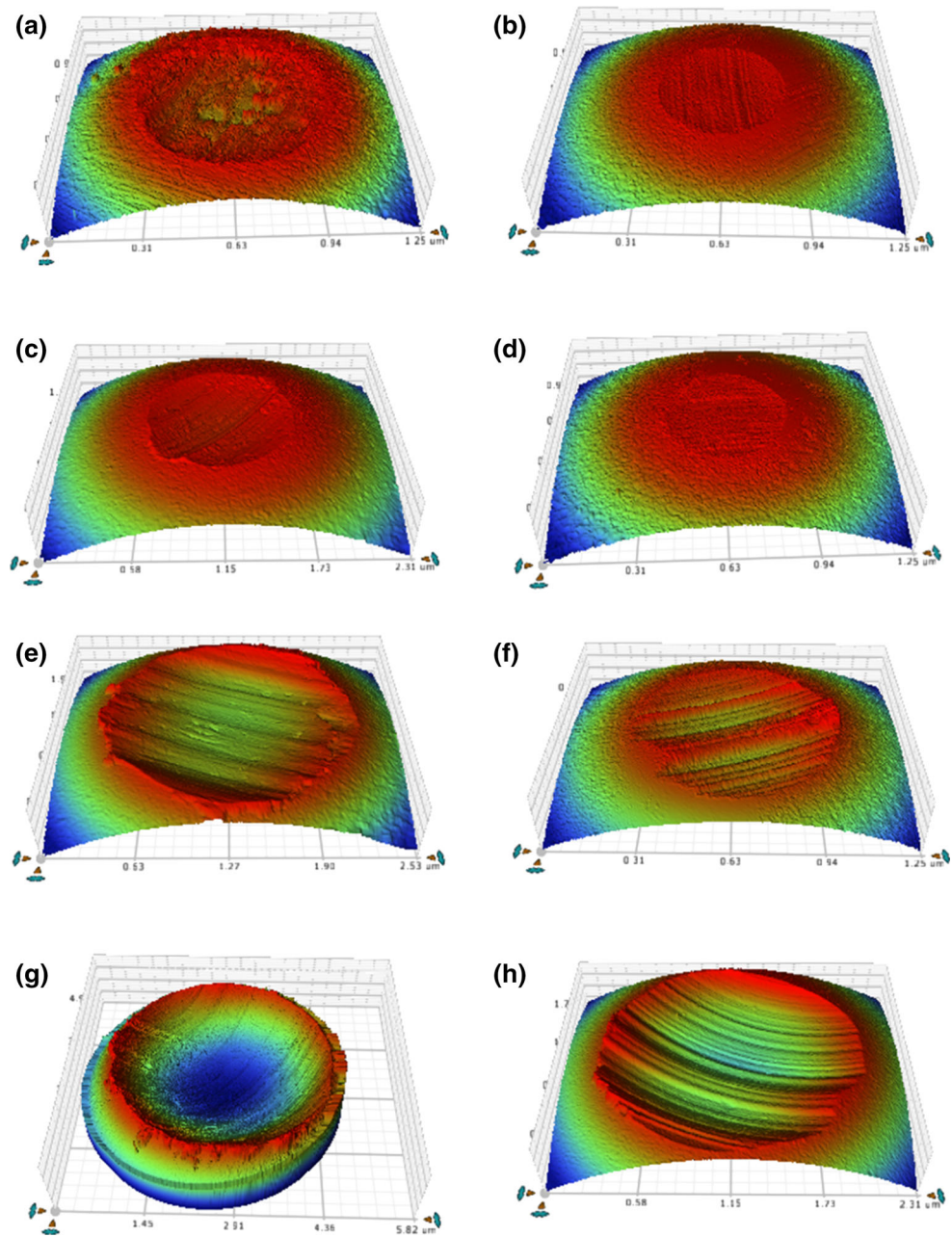


**Fig. 20** SEM micrographs of worn steel ball surfaces lubricated by PAO6 oil **a, c** and PAO6 oil containing 2.0 % of WS<sub>2</sub> nanosheets, **b, d** (load: 392 N; speed: 1200 rev/min; time: 60 min; 150 °C)

**Fig. 21** Three-dimensional morphologies of wear scars lubricated by PAO6 base oil and PAO6-2.0 % WS<sub>2</sub> nanosheets (four-ball machine; load: 392 N, speed 1200 rev/min, time: 60 min): **a** PAO6 at room temperature, **b** PAO6 with 2.0 % WS<sub>2</sub> nanosheets at room temperature, **c** PAO6 at 75 °C, **d** PAO6 with 2.0 % WS<sub>2</sub> nanosheets at 75 °C, **e** PAO6 at 150 °C, **f** PAO6 with 2.0 % WS<sub>2</sub> nanosheets at 150 °C, **g** PAO6 at 200 °C, **h** PAO6 with 2.0 % WS<sub>2</sub> nanosheets at 200 °C



contact region of steel surface, while the atomic concentration of W and O increases from 0.15 and 3.84 % to 3.60 and 16.67 % in the presence of OM-modified WS<sub>2</sub> nanosheets additive. This implies that the OM-modified WS<sub>2</sub> nanosheets additive is absorbed on sliding steel surfaces and partially oxidized during the sliding process.

The worn surfaces of upper steel ball lubricated by PAO6 containing 2.0 % WS<sub>2</sub> nanosheets were analyzed by XPS to acquire more information about the tribochemical reactions involved during the test process. The XPS spectra of C1s, W4p, S2p and Fe2p on the rubbed steel surfaces are shown in Fig. 24 (four-ball machine;

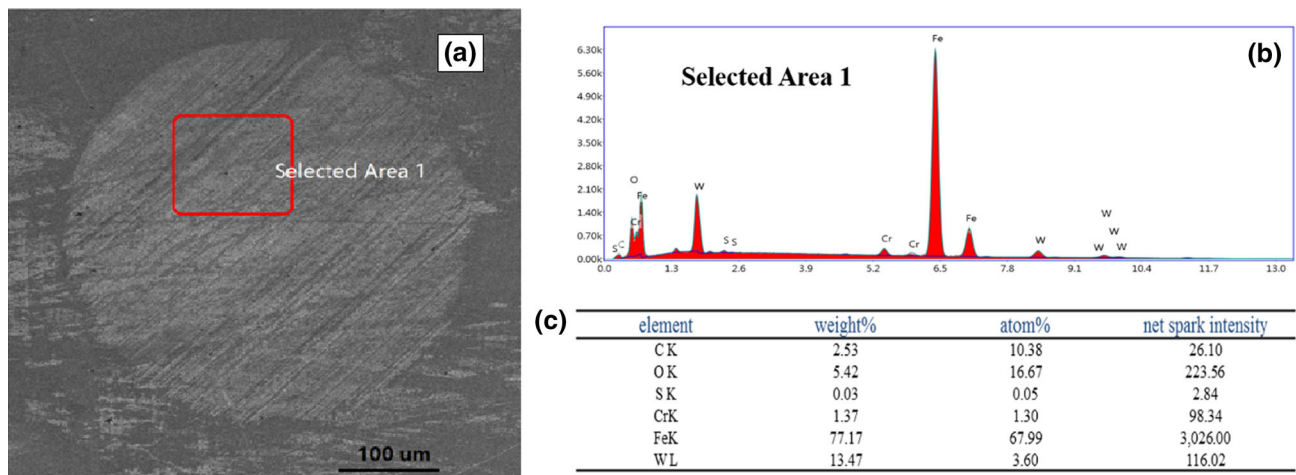


**Fig. 22** SEM image and EDS pattern of the worn surface of lower steel ball lubricated by PAO6-2.0 % WS<sub>2</sub> nanosheets (four-ball machine; load: 392 N, speed 1200 rev/min, time: 60 min, temperature: 75 °C)

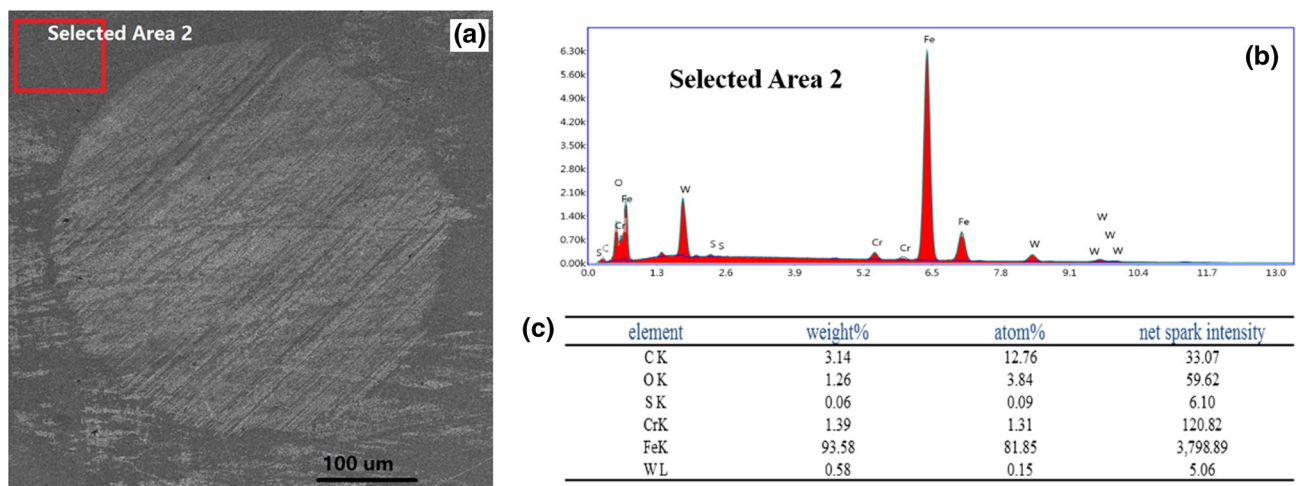


**Fig. 23** SEM image and EDS pattern of the non-contact region of lower steel ball lubricated by PAO6-2.0 % WS<sub>2</sub> nanosheets (four-ball machine; load: 392 N, speed 1200 rev/min, time: 60 min, temperature: 75 °C)

load: 392 N, speed 1200 rev/min, time: 60 min, temperature: 150 °C). A low concentration of S is detected in the tribofilm. The W4f<sub>7/2</sub> and W4f<sub>5/2</sub> peaks correspond to WO<sub>3</sub>, and the Fe2p peaks correspond to iron oxides. This proves that OM-modified WS<sub>2</sub> nanosheets additive is absorbed on sliding steel surface and partially oxidized to form WO<sub>3</sub> during the sliding process. WS<sub>2</sub> nanosheets have a multi-layered structure and relatively weak van der Waals forces that allow the layers to slip under a small shear force, thereby leading to improved lubricating performance [25–27].

Figure 25 schematically shows the tribological model of WS<sub>2</sub> nanosheets in PAO6 base oil. On the one hand, WS<sub>2</sub>

nanosheets with lamellar structure can be deposited on sliding steel surface to form a surface protective and lubricious layer, thereby improving the lubricating performance of the base oil [11, 30]. On the other hand, the OM-modified WS<sub>2</sub> nanosheets can participate in tribochemical reaction to form a tribochemical reaction film composed of WO<sub>3</sub> and iron oxides during the sliding process, thereby improving the tribological properties of the base oil. In terms of the friction-reducing and antiwear abilities, the tribochemical reaction product might be inferior to the surface-modified WS<sub>2</sub> nanosheets, but WS<sub>2</sub> nanosheets as the lubricating oil can comprehensively reduce the friction and wear of the steel–steel contact.

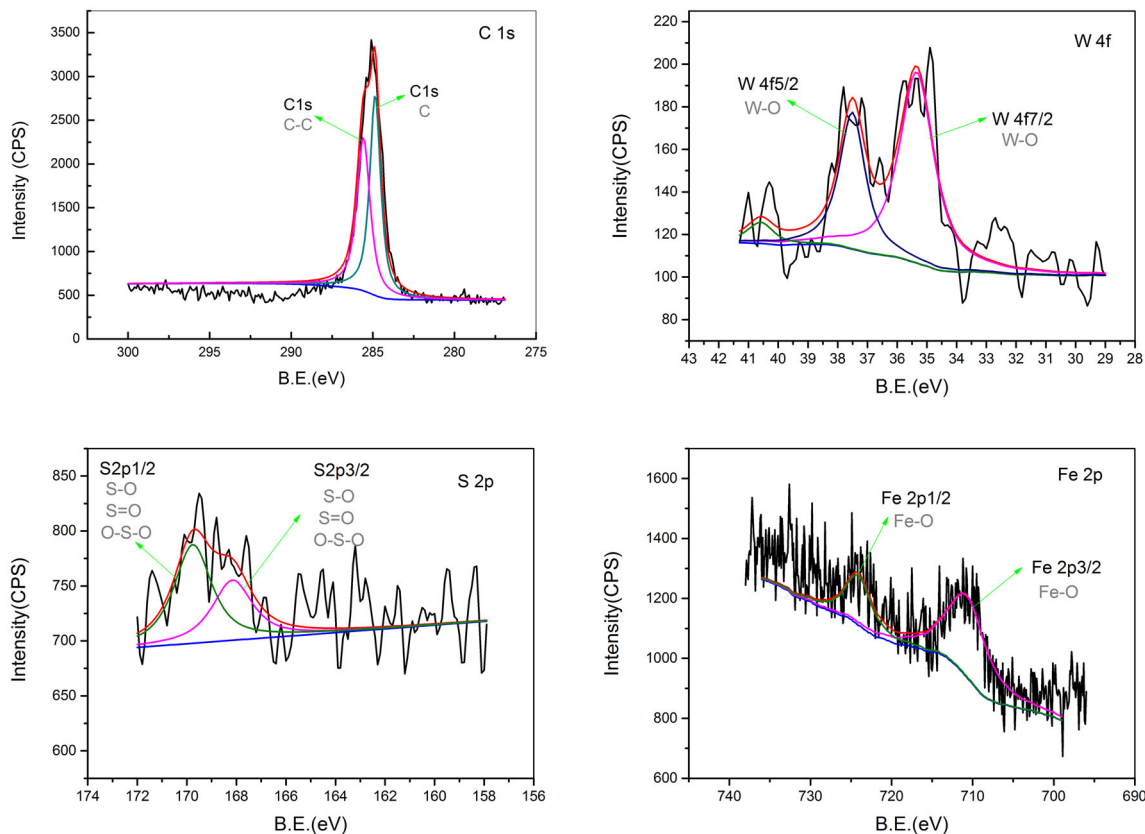
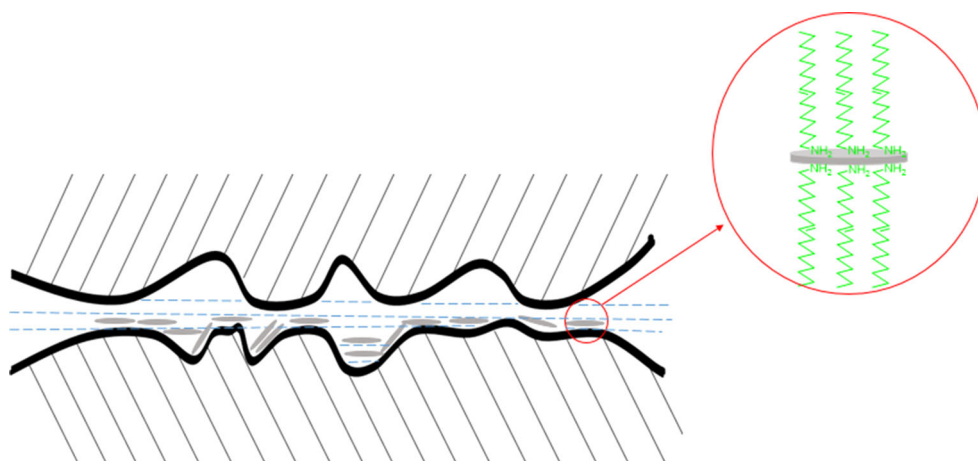


**Fig. 24** XPS spectra of C1 s, W4p, S2p and Fe2p of worn steel ball surfaces lubricated by PAO6 containing 2.0 % WS<sub>2</sub> nanosheets (four-ball machine; load: 392 N, speed 1200 rev/min, time: 60 min, temperature: 150 °C; *B.E.* refers to binding energy)

**Fig. 25** Tribological model of WS<sub>2</sub> nanosheets in the PAO6



**4 Conclusions**

WS<sub>2</sub> nanosheets have been prepared via a solution-phase method at a relatively high temperature of 300 °C. TGA result in combination with the result of rotary oxygen bomb test proves that the as-prepared OM-modified WS<sub>2</sub> nanosheets exhibit good dispersibility in PAO6 base oil and can improve the antioxidation ability of the base oil to

some extent. Friction and wear test data demonstrate that OM-modified WS<sub>2</sub> nanosheets as the additive in PAO6 base oil exhibit excellent friction-reducing and antiwear abilities from room temperature to elevated temperature of 200 °C, showing promising potential as the lubricant additive over a wide temperature range. This is because, as evidenced by relevant SEM-EDS and XPS analyses, WS<sub>2</sub> nanosheets can be well deposited on sliding steel surfaces

to form a surface protective and lubricious layer, while they can also participate in tribochemical reactions to generate tribochemical reaction film composed of  $\text{WO}_3$  and iron oxides on the rubbed steel surfaces, thereby greatly reducing the friction and wear of the steel–steel contact over a wide range of temperature.

**Acknowledgments** The authors acknowledge the financial support provided by the Ministry of Science and Technology of China (Project of “973” plan; Grant No. 2013CB632303), National Natural Science Foundation of China (Grant No. 51275154, 51405132), Plan for Young Scientific Innovation Talent of Henan Province (Grant No. 154100510018), Innovation Scientists and Technicians Troop Construction Projects of Henan Province (C20150011) and Natural Science Foundation of Henan Province (Grant No. 14A15006).

## References

- Amiri, M., Khonsari, M.M.: On the thermodynamics of friction and wear: a review. *Entropy* **12**(5), 1021–1049 (2010). doi:[10.3390/e12051021](https://doi.org/10.3390/e12051021)
- Mo, Y., Tao, D., Wei, X., Li, Q.: Research on friction-coatings with activated ultra-thick tin-base. In: Luo, J., Meng, Y., Shao, T., Zhao, Q. (eds.) *Advanced Tribology*, pp. 915–919. Springer, Berlin Heidelberg (2010)
- Huang, H., Hu, H., Qiao, S., Bai, L., Han, M., Liu, Y., Kang, Z.: Carbon quantum dot/ $\text{CuS}_x$  nanocomposites towards highly efficient lubrication and metal wear repair. *Nanoscale* **7**(26), 11321–11327 (2015). doi:[10.1039/C5NR01923K](https://doi.org/10.1039/C5NR01923K)
- Chen, Y., Zhang, Y., Zhang, S., Yu, L., Zhang, P., Zhang, Z.: Preparation of nickel-based nanolubricants via a facile in situ one-step route and investigation of their tribological properties. *Tribol. Lett.* **51**(1), 73–83 (2013). doi:[10.1007/s11249-013-0148-4](https://doi.org/10.1007/s11249-013-0148-4)
- Yang, G., Zhang, Z., Zhang, S., Yu, L., Zhang, P., Hou, Y.: Preparation and characterization of copper nanoparticles surface-capped by alkanethiols. *Surf. Interface Anal.* **45**(11–12), 1695–1701 (2013). doi:[10.1002/sia.5309](https://doi.org/10.1002/sia.5309)
- Yang, G., Chai, S., Xiong, X., Zhang, S., Yu, L., Zhang, P.: Preparation and tribological properties of surface modified Cu nanoparticles. *Trans. Nonferr. Meta. Soc. China* **22**(2), 366–372 (2012). doi:[10.1016/S1003-6326\(11\)61185-0](https://doi.org/10.1016/S1003-6326(11)61185-0)
- Ingole, S., Charanpahari, A., Kakade, A., Umare, S.S., Bhatt, D.V., Menghani, J.: Tribological behavior of nano  $\text{TiO}_2$  as an additive in base oil. *Wear* **301**, 776–785 (2013). doi:[10.1016/j.wear.2013.01.037](https://doi.org/10.1016/j.wear.2013.01.037)
- Ye, P., Jiang, X., Li, S., Li, S.: Preparation of  $\text{NiMoO}_2\text{S}_2$  nanoparticle and investigation of its tribological behavior as additive in lubricating oils. *Wear* **253**(2), 572–575 (2002). doi:[10.1016/S0043-1648\(02\)00042-X](https://doi.org/10.1016/S0043-1648(02)00042-X)
- Zhang, Z., Xue, Q., Liu, W.: Study on lubricating mechanisms of  $\text{La}(\text{OH})_3$  nanocluster modified by compound containing nitrogen in liquid paraffin. *Wear* **218**(2), 139–144 (1998). doi:[10.1016/S0043-1648\(98\)00225-7](https://doi.org/10.1016/S0043-1648(98)00225-7)
- Chen, S., Liu, W., Yu, L.: Preparation of DDP-coated PbS nanoparticles and investigation of the antiwear ability of the prepared nanoparticles as additive in liquid paraffin. *Wear* **218**(2), 153–158 (1998). doi:[10.1016/S0043-1648\(98\)00220-8](https://doi.org/10.1016/S0043-1648(98)00220-8)
- Winer, W.O.: Molybdenum disulfide as a lubricant: a review of the fundamental knowledge. *Wear* **10**(6), 422–452 (1967). doi:[10.1016/0043-1648\(67\)90187-1](https://doi.org/10.1016/0043-1648(67)90187-1)
- Drummond, C., Alcantar, N., Israelachvili, J., Tenne, R., Golan, Y.: Microtribology and friction-induced material transfer in  $\text{WS}_2$  nanoparticle additives. *Adv. Funct. Mater.* **11**(5), 348–354 (2001). doi:[10.1002/1616-3028\(200110\)11:5<348:AID-ADFM348>3.0.CO;2-S](https://doi.org/10.1002/1616-3028(200110)11:5<348:AID-ADFM348>3.0.CO;2-S)
- Ratoi, M., Niste, V., Walker, J., Zekonyte, J.: Mechanism of action of  $\text{WS}_2$  lubricant nanoadditives in high-pressure contacts. *Tribol. Lett.* **52**(1), 81–91 (2013). doi:[10.1007/s11249-013-0195-x](https://doi.org/10.1007/s11249-013-0195-x)
- Aldana, P., Vacher, B., Le Mogne, T., Belin, M., Thiebaut, B., Dassenoy, F.: Action mechanism of  $\text{WS}_2$  nanoparticles with ZDDP additive in boundary lubrication regime. *Tribol. Lett.* **56**(2), 249–258 (2014). doi:[10.1007/s11249-014-0405-1](https://doi.org/10.1007/s11249-014-0405-1)
- Ratoi, M., Niste, V.B., Zekonyte, J.:  $\text{WS}_2$  nanoparticles—potential replacement for ZDDP and friction modifier additives. *RSC Adv.* **4**(41), 21238–21245 (2014). doi:[10.1039/C4RA01795A](https://doi.org/10.1039/C4RA01795A)
- Joly-Pottuz, L., Dassenoy, F., Belin, M., Vacher, B., Martin, J.M., Fleischer, N.: Ultralow-friction and wear properties of IF- $\text{WS}_2$  under boundary lubrication. *Tribol. Lett.* **18**(4), 477–485 (2005). doi:[10.1007/s11249-005-3607-8](https://doi.org/10.1007/s11249-005-3607-8)
- Greenberg, R., Halperin, G., Etsion, I., Tenne, R.: The effect of  $\text{WS}_2$  nanoparticles on friction reduction in various lubrication regimes. *Tribol. Lett.* **17**(2), 179–186 (2004). doi:[10.1023/B:TRIL.0000032443.95697.1d](https://doi.org/10.1023/B:TRIL.0000032443.95697.1d)
- Rapoport, L., Leshchinsky, V., Lapsker, I., Volovik, Y., Nepomnyashchy, O., Lvovsky, M., Popovitz-Biro, R., Feldman, Y., Tenne, R.: Tribological properties of  $\text{WS}_2$  nanoparticles under mixed lubrication. *Wear* **255**(7–12), 785–793 (2003). doi:[10.1016/S0043-1648\(03\)00044-9](https://doi.org/10.1016/S0043-1648(03)00044-9)
- Rapoport, L., Lvovsky, M., Lapsker, I., Leshchinsky, W., Volovik, Y., Feldman, Y., Tenne, R.: Friction and wear of bronze powder composites including fullerene-like  $\text{WS}_2$  nanoparticles. *Wear* **249**(1–2), 149–156 (2001). doi:[10.1016/S0043-1648\(01\)00519-1](https://doi.org/10.1016/S0043-1648(01)00519-1)
- An, V., Irtegov, Y., de Izarra, C.: Study of tribological properties of nanolamellar  $\text{WS}_2$  and  $\text{MoS}_2$  as additives to lubricants. *J. Nanomater.* **2014**, 8 (2014). doi:[10.1155/2014/865839](https://doi.org/10.1155/2014/865839)
- Twist, C., Bassanetti, I., Snow, M., Delferro, M., Bazzi, H., Chung, Y.-W., Marchió, L., Marks, T., Wang, Q.J.: Silver-organic oil additive for high-temperature applications. *Tribol. Lett.* **52**(2), 261–269 (2013). doi:[10.1007/s11249-013-0211-1](https://doi.org/10.1007/s11249-013-0211-1)
- ASTM International: Evaluation of automotive engine oils in the sequence IIIG, spark-ignition engine. In: *ASTM Book of Standards*, pp. 1–49. ASTM International, West Conshohocken (2012)
- Cheng, L., Huang, W., Gong, Q., Liu, C., Liu, Z., Li, Y., Dai, H.: Ultrathin  $\text{WS}_2$  nanoflakes as a high-performance electrocatalyst for the hydrogen evolution reaction. *Angew. Chem. Int. Ed.* **53**(30), 7860–7863 (2014). doi:[10.1002/ange.201405193](https://doi.org/10.1002/ange.201405193)
- Lee, C., Hwang, Y., Choi, Y., Lee, J., Choi, C., Oh, J.: A study on the tribological characteristics of graphite nano lubricants. *Int. J. Precis. Eng. Manuf.* **10**(1), 85–90 (2009). doi:[10.1007/s12541-009-0013-4](https://doi.org/10.1007/s12541-009-0013-4)
- Greenwood, O.D., Moulzolf, S.C., Blau, P.J., Lad, R.J.: The influence of microstructure on tribological properties of  $\text{WO}_3$  thin films. *Wear* **232**(1), 84–90 (1999). doi:[10.1016/S0043-1648\(99\)00255-0](https://doi.org/10.1016/S0043-1648(99)00255-0)
- Fan, X., Wang, L., Li, W., Wan, S.: Improving tribological properties of multialkylated cyclopentanes under simulated space environment: two feasible approaches. *ACS Appl. Mater. Interfaces* **7**(26), 14359–14368 (2015). doi:[10.1021/acsami.5b03088](https://doi.org/10.1021/acsami.5b03088)
- Si, P.Z., Choi, C.J., Lee, J.W., Geng, D.Y., Zhang, Z.D.: Synthesis, structure and tribological performance of tungsten disulphide nanocomposites. *Mater. Sci. Eng. A* **443**(1–2), 167–171 (2007). doi:[10.1016/j.msea.2006.08.026](https://doi.org/10.1016/j.msea.2006.08.026)
- Moshkovith, A., Perfiliev, V., Lapsker, I., Fleischer, N., Tenne, R., Rapoport, L.: Friction of fullerene-like  $\text{WS}_2$  nanoparticles:

- effect of agglomeration. *Tribol. Lett.* **24**(3), 225–228 (2006). doi:[10.1007/s11249-006-9124-6](https://doi.org/10.1007/s11249-006-9124-6)
29. Kheireddin, B.A., Lu, W., Chen, I.C., Akbulut, M.: Inorganic nanoparticle-based ionic liquid lubricants. *Wear* **303**(1–2), 185–190 (2013). doi:[10.1016/j.wear.2013.03.004](https://doi.org/10.1016/j.wear.2013.03.004)
30. Martin, J.M.: Molybdenum disulphide lubrication: Lansdown, A.R. *Tribology series*, 35, Dowson, D. (Ed.) 1999, pp. 380. *Tribol. Int.* **33** (2), 148–149 (2000). doi:[10.1016/S0301-679X\(00\)00020-7](https://doi.org/10.1016/S0301-679X(00)00020-7)